Macromolecules

Article

Cite This: Macromolecules 2018, 51, 7828−7835

pubs.acs.org/Macromolecules

Side Chain Effects on the Optoelectronic Properties and Self-Assembly Behaviors of Terthiophene−Thieno[3,4-*c*]pyrrole-4,6-dione Based Conjugated Polymers

Chien-An Chen,[†] Po-Chih Yang,[‡] Shih-Chieh Wang,[‡] Shih-Huang Tung,[†] and Wei-Fang Su*[,‡]

[†]Institute of Polymer Science and Engineering and [‡]Department of Materials Science and Engineering, National Taiwan University, Taipei, Taiwan 10617

Supporting Information

ABSTRACT: The donor−acceptor conjugated polymers (CPs) of terthiophene−thieno[3,4-*c*]pyrrole-4,6-dione (3T-TPD) are widely used to fabricate low-cost flexible electronics. We present a comprehensive study of the side chain effect on the optical properties, electrochemical properties, thermal properties, and self-assembly behavior of 3T-TPD CPs, including side chain location (outward vs inward), type (tetraethylene glycol (TEG) vs dodecyl), and length (octyl vs hexyl vs butyl). For the side chain location effect, the polymers with outward side chains show better coplanarity of backbone than the polymers with inward side chains, leading to form lamellae structure. However, interestingly, the inward series polymers exhibit novel hexagonal structure. Through replacing dodecyl chains with TEG chains and changing the side chain length, ultrahigh ordered lamellae and hexagonal structure can be obtained. Furthermore, two models are purposed to explain the formation mechanism of lamellae and hexagonal structure. This study can provide a strategy to design the CPs with highly ordered nanostructures.

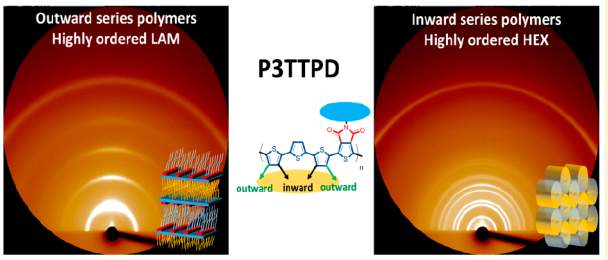

INTRODUCTION

The donor−acceptor conjugated polymers (CPs) have been widely used to fabricate organic field-effect transistors (OFETs), polymer solar cells (PSCs), sensors, and so on. These optoelectronic devices have potential for replacing inorganic material based devices due to their lightweight, flexible characteristics, and rapid energy payback time and are suitable for low-cost roll-to-roll processing.[1−5]

In the development of conjugated polymers, many donors and acceptors are used to construct donor−acceptor alternating CPs. The examples of donors, oligothiphene,[6] benzodithiophene,[7,8] cyclopentadithiophene,[9,10] selenophene,[11,12] carbazole,[13] etc., have been studied. The examples of acceptors, benzothiadiazole,[14] isoindigo,[15] pyrrolo[3,4-*c*]pyrrole-1,4- dione (DPP),[16] thieno[3,4-*c*]pyrrole-4,6-dione (TPD),[17,18] bithiopheneimide (BTI),[19,20] etc., have been investigated. In this study, we focus on terthiophene(3T)-TPD based CPs (P3TTPD) to investigate the side chain effects on their optoelectronic properties and self-assembly behaviors due to the merits of their characteristics of easy synthesis, air stability, and good device performance (OFET: $\mu_h \sim 1$ cm^2/(V·s); PSC: power conversion efficiency ~8%).[17,18]

The donor−acceptor alternating CPs consist of two parts: main chain and side chain. The main chain is made of stiff π-conjugated bond, and the side chain is usually built on a flexible nonconjugated bond. The main chain has the active functions of light absorption and charge transportation. On the other hand, the side chain enables the polymer to dissolve and disperse in organic solvent and enhance the organization and crystallization of polymer. The "side chain engineering" is a technique to tune the chemical and physical properties and to improve the device performance of the conducting polymer. The technique usually involves three parameters: side chain location,[21] side chain type,[22−25] and side chain length.[26−28] Many types of chemical structure have been investigated including alkyl side chains,[22] hybrid side chains,[29] ionic side chains,[23] oligoether side chains,[25,30] fluoroalkyl side chains,[31] and latent reactive side chains.[32] Among these side chains, oligoether side chains attracted lots of attention because they are more flexible as compared with alkyl side chains and enable the polymer to be dissolved in environment-friendly solvent.[24]

In 2013, Leclerc et al. were the first to introduce an oligoether chain into the P3TTPD system. They successfully synthesized an amphiphilic donor−acceptor CP that can be fabricated into a Langmuir−Blodgett film.[33] In 2015, Marks et al. systematically studied side chain location effect on the properties of P3TTPD based polymers.[17] The results showed that the location of side chain can significantly influence the coplanarity and the crystallinity of the polymer, leading to affect the performance of the devices. However, a systematic study of side chain effects of aforementioned three parameters has not been performed in the literature.

Received: May 22, 2018
Revised: September 12, 2018
Published: September 26, 2018

DOI: 10.1021/acs.macromol.8b01073
Macromolecules 2018, 51, 7828−7835

Scheme 1. Chemical Structures of Eight P3TTPD Polymers

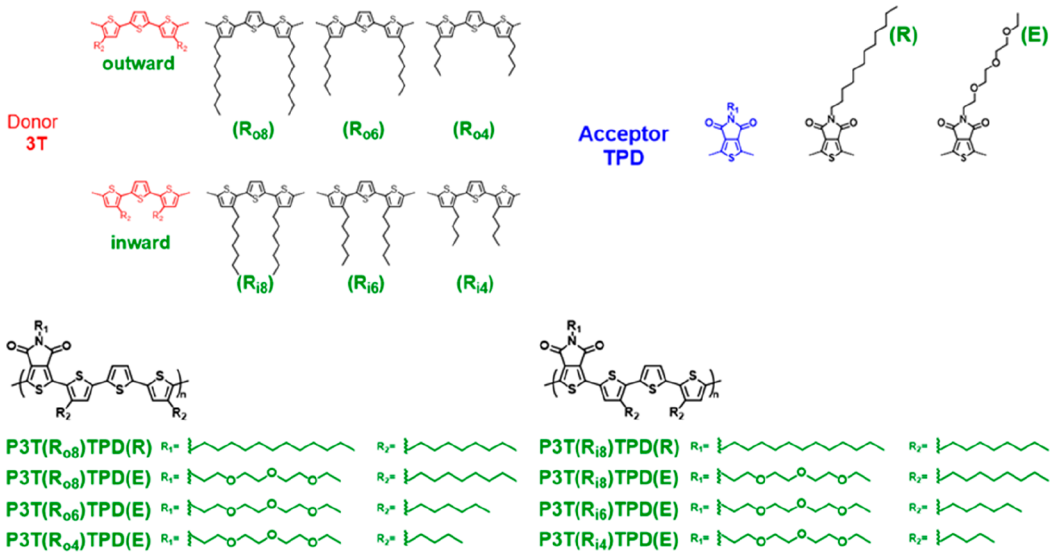

Herein, we present a comprehensive study of side chain effects for P3TTPD system including location, type, and length. The detailed results and discussion are present below. This study provides a strategy to design conjugating polymers with highly ordered lamella and hexagonal nanostructures for potential applications in high performance optoelectronics.

RESULTS AND DISCUSSION

We synthesized eight P3TTPD polymers with two side chains on the 3T unit by varying their location (outward and inward), types on the TPD unit (dodecyl and tetraethylene glycol (TEG)), and three different lengths on the 3T unit (octyl, hexyl, and butyl), as shown in Scheme 1. They are named P3T(R_{in})TPD(R), P3T(R_{in})TPD(E), P3T(R_{on})TPD(R), and P3T(R_{on})TPD(E), where "R" is the alkyl side chain and "E" is the oligoether side chain, "i" represents the two R located at the 3,3″-position of 3T (inward), "o" represents the two R located at the 4,4″-position of 3T (outward), and "*n*" is the length of R. The synthesis, characterization, and self-assembly of the polymers are discussed in the following sections.

Polymer Synthesis. A detailed synthesis scheme for the P3TTPD polymers is shown in the Supporting Information. The monomers were purified by distillation, column chromatography, and recrystallization to ensure their purity of >95% determined by ^{1}H nuclear magnetic resonance (^{1}H NMR). The polymers were synthesized by the Stille coupling reaction using $Pd_2(dba)_3$ catalyst and P(o-tol)$_3$ ligand using a microwave reactor. The polymers were purified via multiple Soxhlet extractions. The molecular weights of these polymers were measured by gel permeation chromatography (GPC), and the results are summarized in Table 1. To study the chain length effect of side chain without the issue of chain entanglement, we synthesized polymers containing relative short side chain (≤8 carbons), so their solubility is low, especially the four-carbon length. To avoid the molecular weight effect in this study, we synthesized the polymers with similar molecular weight in the range 3−7 kDa.

Optical Properties. Figure 1 shows the film absorption spectra of synthesized polymers. The λ_{max} and bandgap of the films are summarized in Table 1. For the side chain location effect, the polymer with outward side chains (P3T(R_{o8})TPD(R)) shows a red-shift of λ_{max} (529 nm vs 507 nm) and a higher absorption of $\lambda_{shoulder}$ than the polymer with inward side chains (P3T(R_{i8})TPD(R)) when the polymers consists of an octyl group on the 3T unit and a dodecyl on the TPD unit. The results signify that P3T(R_{o8})TPD(R) has better molecular packing than P3T(R_{i8})TPD(R). We used the frontier molecular orbital computation to determine the coplanarity of backbone of each polymer; only one unit was utilized to save computation time (Figure S2 of the Supporting Information). The figure shows that the outward polymer, P3T(R_{o8})TPD(R), has higher coplanarity and smaller torsion angle of 3T than the inward polymer, P3T(R_{i8})TPD(R), for better packing (Table S2). For the side chain type effect (TEG vs dodecyl), the side chains on the 3T unit are fixed as octyl; the polymer with an oligoether side chain shows longer wavelength of λ_{max} than the polymer with the alkyl side chain. Furthermore, for outward series polymers, the P3T(R_{o8})TPD(E) shows a longer wavelength of λ_{max} (573 nm vs 529 nm, red-shift: 44 nm) as compared with P3T(R_{o8})TPD(R). For inward series polymers, P3T(R_{i8})TPD(E) also shows a larger red-shift λ_{max} (510 nm vs 507 nm, red-shift: 3 nm) than P3T(R_{i8})TPD(R). In comparison, the red-shifted amount of

Table 1. Summary of Molecular Weights and Optical Properties for P3TTPD Polymers

polymer	M_n (kDa)[a]	PDI[a]	λ_{max} (nm)[b]	$\lambda_{shoulder}$ (nm)[b]	E_g^{opt} (eV)[c]
P3T(R_{o8})TPD(R)	3.65	1.57	529	618	1.86
P3T(R_{o8})TPD(E)	7.06	2.10	573	671	1.85
P3T(R_{o6})TPD(E)	4.69	2.04	567	671	1.85
P3T(R_{o4})TPD(E)	4.23	1.82	562	667	1.86
P3T(R_{i8})TPD(R)	4.07	1.15	507		1.72
P3T(R_{i8})TPD(E)	6.09	1.13	510		1.72
P3T(R_{i6})TPD(E)	4.08	1.17	513		1.71
P3T(R_{i4})TPD(E)	3.11	1.20	517		1.72

[a]Molecular weight of the polymers estimated from GPC using polystyrene standard, chloroform as eluent, at 40 °C. [b]UV−vis absorption spectra of films were measured using spun-cast film from 10 mg/mL chloroform solutions. [c]Optical bandgap of each film was calculated from its absorption edge (onset of the peak) of the UV−vis spectrum.

DOI: 10.1021/acs.macromol.8b01073
Macromolecules 2018, 51, 7828−7835

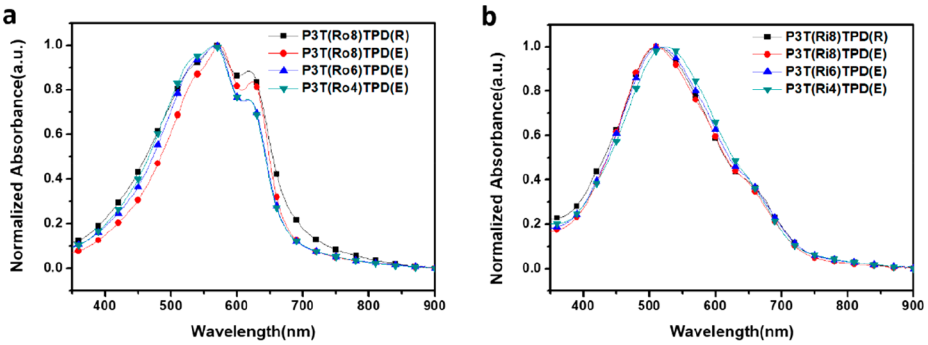

Figure 1. Optical absorption spectra of (a) outward series polymer (P3T(R_{on})TPD(R, E)) films and (b) inward series polymer (P3T(R_{in})TPD(R, E)) films spun-cast from 10 mg/mL chloroform solutions.

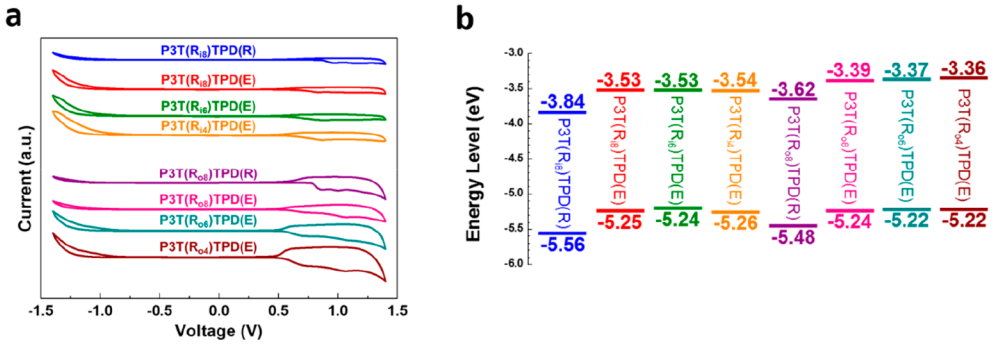

Figure 2. (a) Cyclic voltammetry spectra and (b) schematic diagram of energy level of synthesized polymers.

λ_{max} is more significant in outward series polymers (44 nm) than in inward series polymers (3 nm). All above results indicate that the oligoether side chain is more effective on the packing of polymers than the alkyl side chain due to the presence of an oxygen atom having more spatial space for self-assembly.[34]

The side chain length effect was investigated by reducing from octyl to hexyl and butyl side chains on the 3T unit when the side chain on TPD unit is fixed as TEG. For outward series polymers, the polymer with longest side chain (P3T(R_{o8})-TPD(E)) shows the longest wavelength of λ_{max} (573 nm), which indicates that the molecular packing and self-assembly of polymer are increased with increasing side chain length. On the contrary, for the inward series polymers, the polymer with the shortest side chain (P3T(R_{i4})TPD(E)) shows the longest wavelength of λ_{max} (517 nm). That reveals the self-assembly behavior of the polymer is improved with decreasing side chain length. More detailed discussions on the structural formation mechanism using the model will be present in a later section to explain the differences of self-assembly behaviors among the P3T-TPD polymers.

The optical bandgaps of the polymers are calculated by the formula, $1240/\lambda_{onset}$, where λ_{onset} is the onset of absorption peak with longest wavelength. For the polymer with the outward side chains, the polymers have a similar bandgap of 1.85−1.86 eV (Table 1). In comparison, the inward series polymers have a lower band gap of 1.71−1.72 eV than the outward series polymers. In addition, the type and length of side chain do not significantly influence the bandgap of the polymers. In general, for the polymer with a better packing, the bandgap of the polymer is smaller.[15] However, we observed that the inward series polymers, known to have poor packing, exhibit a smaller bandgap than the outward series polymers. This interesting result may be related to the extended conjugating length of inward series polymers. Detailed discussions will be presented in the later section of morphology.

Electrochemical Properties. Figure 2 shows cyclic voltammetry spectra of all polymers and schematic diagram of energy level of synthesized polymers. Every polymer shows clear oxidation peak at oxidation conditions (0 V → 1.4 V → 0 V). However, no significant peak is observed for each polymer at reduction condition (0 V → −1.4 V → 0 V). The results indicate every polymer is p-type. The HOMO and LUMO energy levels of each polymer were calculated using the following formulas:

$$\text{HOMO} = -\{E_{oxi} - E_{Fc/Fc^+} + 5.13\}\ \text{eV}$$

$$\text{LUMO} = -\text{HOMO} + E_g^{opt}$$

where E_{oxi}, E_{Fc/Fc^+}, and E_g^{opt} are the oxidation potential of the polymer, oxidation potential of the ferrocene as standard, and bandgap value obtained from the UV−vis spectrum of the polymer, respectively. For the side chain location effect, the outward series polymer, P3T(R_{o8})TPD(R), shows a higher energy level (HOMO: −5.48 eV vs −5.56 eV, LUMO: −3.62 eV vs −3.84 eV) than the polymers with inward side chains, P3T(R_{i8})TPD(R). The results are due to better coplanarity of the backbone of P3T(R_{o8})TPD(R) than that of P3T(R_{i8})-TPD(R), which promotes electrons to be delocalized easily. By comparison of the TEG(E) chain with the dodecyl(R) chain, for outward series polymers, P3T(R_{o8})TPD(E) shows a higher energy level (HOMO: −5.24 eV vs −5.48 eV; LUMO: −3.39 eV vs −3.62 eV) than that of P3T(R_{o8})TPD(R). The same trend is also found in inward series polymers. These results are attributed to the stronger electron donating ability of TEG

DOI: 10.1021/acs.macromol.8b01073
Macromolecules 2018, 51, 7828−7835

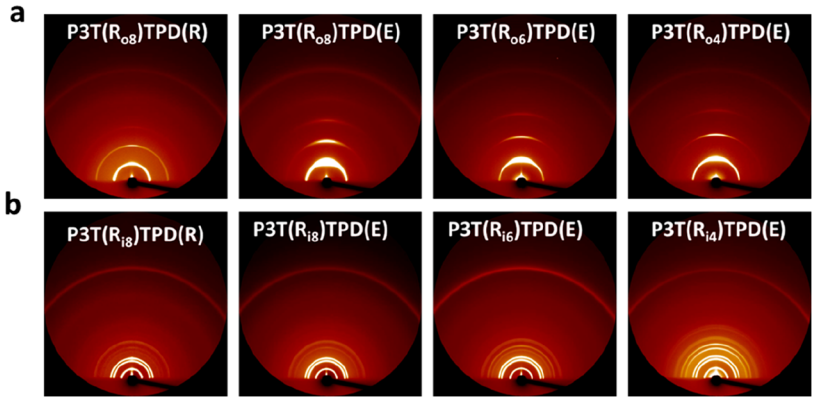

Figure 3. 2D patterns of GIWAXS of (a) outward series polymers and of (b) inward series polymers.

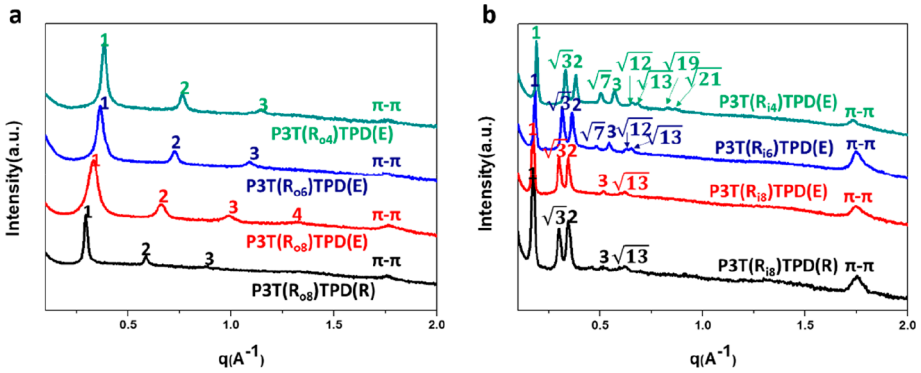

Figure 4. Line cut data of GIWAXS of (a) outward series polymers and of (b) inward series polymers.

Table 2. Summary of GIWAXS Parameters of the Polymer Films

polymer	*d*-spacing (Å)	$d_{\pi-\pi}$ (Å)	peak ratio	structure
P3T(R$_{o8}$)TPD(R)	21.4	3.6	1:2:3	LAM
P3T(R$_{o8}$)TPD(E)	19.0	3.6	1:2:3:4	LAM
P3T(R$_{o6}$)TPD(E)	17.3	3.6	1:2:3	LAM
P3T(R$_{o4}$)TPD(E)	16.4	3.6	1:2:3	LAM
P3T(R$_{i8}$)TPD(R)	36.7	3.6	1:$\sqrt{3}$:2:3:$\sqrt{13}$	HEX
P3T(R$_{i8}$)TPD(E)	36.7	3.6	1:$\sqrt{3}$:2:3:$\sqrt{13}$	HEX
P3T(R$_{i6}$)TPD(E)	34.9	3.6	1:$\sqrt{3}$:$\sqrt{7}$:2:3:$\sqrt{12}$:$\sqrt{13}$	HEX
P3T(R$_{i4}$)TPD(E)	33.4	3.6	1:$\sqrt{3}$:2:$\sqrt{7}$:3:$\sqrt{12}$:$\sqrt{13}$:$\sqrt{19}$:$\sqrt{21}$	HEX

chain than that of dodecyl chain. Furthermore, the side chain length (octyl vs hexyl vs butyl) on the 3T moiety marginally affects the energy level of the polymers as shown in Figure 2b. The differences on the electron donating ability of different lengths of alkyl chains are not significant.[26]

Thermal Properties. TGA profiles of synthesized polymers are shown in Figure S4. The TGA data are summarized in Table S4. The outward series polymer, P3T(R$_{o8}$)TPD(R), shows T_d of 416 °C. The T_d is decreased to 393 °C by replacing the dodecyl chain with a TEG chain. The inward series polymers also show the same trend (436 °C → 383 °C). These results are due to that reactive oxygen radicals induce the polymer to be dissociated easily. There is no significant trend by varying the side chain length from octyl to hexyl and butyl. Even though TEG chain reduces the thermal stability of the polymers, all synthesized polymers still show a high T_d over 350 °C. The DSC profiles of synthesized polymers are shown in Figure S5, and relevant data are summarized in Table S4. The outward series polymers show obvious melting peaks. However, no significant peak is observed in inward series polymers. These results indicate that outward series polymers have better packing than inward series polymers due to the higher degree of coplanarity. The outward series polymer, P3T(R$_{o8}$)TPD(R), shows a T_m of 239 °C. The T_m is increased to 296 °C by replacing the dodecyl chain with a TEG chain. These results indicate that the more flexible TEG chain helps the outward series polymer to pack into highly ordered nanostructure. Furthermore, the T_m is decreased from 296 °C to 266 °C to 247 °C by changing the octyl to hexyl to butyl. This result reveals that the outward series polymers pack into highly ordered nanostructure with increased side chain length. The longer side chain provides more mobility than the shorter side chain during the self-assembly process. All results of DSC are in agreement with the results of UV−vis spectra.

Morphology Study. Figure 3 shows 2D patterns of grazing-incidence wide-angle X-ray scattering (GIWAXS) of the film of synthesized polymers. The outward series polymer, P3T(R$_{o8}$)TPD(R), shows random orientation. By replacement of the dodecyl(R) chain with a TEG(E) chain, P3T(R$_{o8}$)-TPD(E) shows an edge-on orientation. The orientation

DOI: 10.1021/acs.macromol.8b01073
Macromolecules 2018, 51, 7828−7835

remains by varying the side chain length. However, inward series polymers show a random orientation. To investigate the nanostructures of polymers, the line cut data of GIWAXS are shown in Figure 4. The relevant data are summarized in Table 2.

In outward series polymers (Figure 4a), P3T(R_{o8})TPD(R) shows multiple scattering peaks in the ratio of 1:2:3, a typical scattering pattern for ordered lamellae (LAM) structure, and one peak in the high q region (q > 1.5 Å^{-1}) which presents $\pi-\pi$ stacking. The d-spacing and $d_{\pi-\pi}$ are 21.4 Å and 3.6 Å, respectively. For the side chain type effect (TEG vs dodecyl), P3T(R_{o8})TPD(E) shows more scattering peaks in the ratio of 1:2:3:4 than P3T(R_{o8})TPD(R). The result indicates that P3T(R_{o8})TPD(E) can self-assemble into higher order LAM structure than P3T(R_{o8})TPD(R) because E is more flexible than R. For P3T(R_{o8})TPD(E), the d-spacing and $d_{\pi-\pi}$ are 19.0 Å and 3.6 Å, respectively. The d-spacing of the polymer decreased by 2.4 Å by replacing the alkyl chain with a TEG chain, signifying that the TEG chain occupies smaller spacing than the alkyl chain even though the amounts of atoms in the chain are similar (TEG: 11 atoms; alkyl chain: 12 atoms). These results suggest that the flexible TEG chain having larger spatial space in outward series polymers can dramatically improve the self-assembly behavior and change orientation from random to edge-on. Furthermore, by decreasing from octyl to hexyl to butyl, the d-spacing of the polymer becomes smaller from 19.0 Å to 17.3 Å to 16.4 Å, but the regularity of its nanostructure is reduced. Therefore, in outward series polymers, P3T(R_{o8})TPD(E) shows the highest order of LAM structure.

In inward series polymers (Figure 4b), P3T(R_{i8})TPD(R) shows multiple scattering peaks in the ratio of $1:\sqrt{3}:2:3:\sqrt{13}$, a typical scattering pattern for ordered hexagonal (HEX) structure, and one peak in the high q region. The d-spacing and $d_{\pi-\pi}$ are 36.7 Å and 3.6 Å, respectively. This special HEX structure is rarely found in donor−acceptor alternating CPs. The formation mechanism will be discussed later using the model. For the side chain type effect (TEG vs dodecyl), in the inward polymers, both side chains show similar order of HEX structure, so the effect is not obvious. However, the effect of side chain length on the self-assembly behavior of inward polymers is quite large (octyl vs hexyl vs butyl); the regularity of HEX is dramatically enhanced with decreased side chain length. Hence, the shortest side chain inward polymer, P3T(R_{i4})TPD(E), shows the highest order of HEX structure with scattering peaks in the ratio of $1:\sqrt{3}:2:\sqrt{7}:3:\sqrt{12}:\sqrt{13}:\sqrt{19}:\sqrt{21}$.

In general, the $d_{\pi-\pi}$ (distance of backbone packing) of conducting polymer is influenced by the steric effect from the size of the side chain. It is interesting to note that the $d_{\pi-\pi}$ does not change at all among the synthesized polymers. This result indicates that the $d_{\pi-\pi}$ is determined by the large side chain on the "TPD" unit rather than the small side chains on 3T unit (octyl, hexyl, and butyl). Even though TEG occupied smaller space than dodecyl, the size difference in one atom between them does not provide enough steric effect to affect $d_{\pi-\pi}$. Therefore, all synthesized polymers with TEG or dodecyl on TPD acceptor show the same value of $d_{\pi-\pi}$ regardless of the side chain length on the 3T donor.

In a short summary, the outward series polymers self-assemble into LAM, and inward series polymers having curvature structure self-assemble into HEX. The polymers with a TEG chain show higher order of nanostructure than the polymers with a dodecyl chain because the TEG chain is more flexible than the alkyl chain. Thus, the TEG chain is more effective to assist the self-assembly of the outward series polymers than that of the inward series polymers. In outward series polymers, the highest order of LAM can be achieved with the longest side chain. On the contrary, in inward series polymers, the polymer with the shortest side chain shows the highest order of HEX. Both data of GIWAXS and UV−vis provide the information about molecular packing, and they are in good agreement. The contradictory results of the side chain length effect between inward series polymers and outward series polymer will be discussed later using the model.

The two polymers P3T(R_{o8})TPD(E) and P3T(R_{i4})TPD(E) exhibit the highest order of LAM and HEX, respectively, among the eight synthesized polymers. Figure 5 shows their

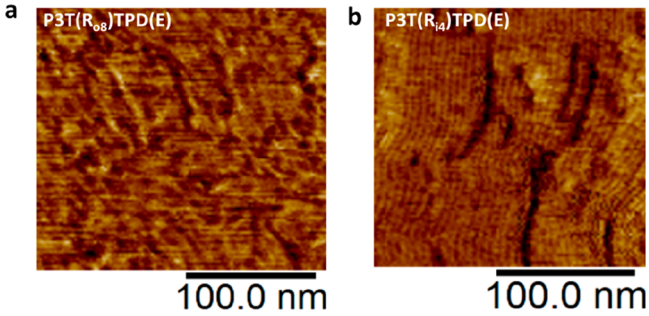

Figure 5. Two representative phase images of (a) P3T(R_{o8})TPD(E) and (b) P3T(R_{i4})TPD(E) with the most ordered LAM and HEX, respectively, among the eight synthesized polymers.

AFM images. According to the results of 2D-GIWAXS, P3T(R_{o8})TPD(E) shows an edge-on orientation, so the arrangement of lamellar layer is parallel to the substrate. Hence, the surface morphology of P3T(R_{o8})TPD(E) is flat with less feature as shown in Figure 5a. The AFM image of P3T(R_{i4})TPD(E) exhibits alternating bright and dark straps which indicate hard segments and soft segments, respectively, as shown in Figure 5b. This pattern is a kind of HEX pattern. The length of each polymer chain is about 1 nm estimated from its molecular weight. Furthermore, these straps are straight, and their length is over 500 nm. We speculated the strap is made from polymer bundles. Every polymer bundle resulted from the self-assembled polymer backbone about 1 nm, estimated from its molecular weight. Such long and straight straps reveal that conjugated length of the polymer is extended by well attached polymer bundles as shown in Figure S6. Thus, the extended conjugating length of inward series polymers exhibits a smaller bandgap as compared with outward series polymers. Other AFM images of the films of synthesized polymers are shown in Figure S3.

Model for Self-Assembly Behavior. We propose two models to explain the formation lamella structure (LAM) from P3T(R_{o8})TPD(E) and hexagonal structure (HEX) from P3T(R_{i4})TPD(E), as shown in Figure 6. One usually expects the formation of lamella structure from conducting polymers due to their rigid rod characteristics.[15,35,36] From the above discussion, we can conclude that the outward series polymers have better coplanarity in the backbone and pack the polymer chains better as compared with inward series polymers. Many backbones of the polymers can pack into a long-range lamellar layer with side chains sticking out straight and further self-assemble into lamellar structure. Therefore, the longer side

DOI: 10.1021/acs.macromol.8b01073
Macromolecules 2018, 51, 7828−7835

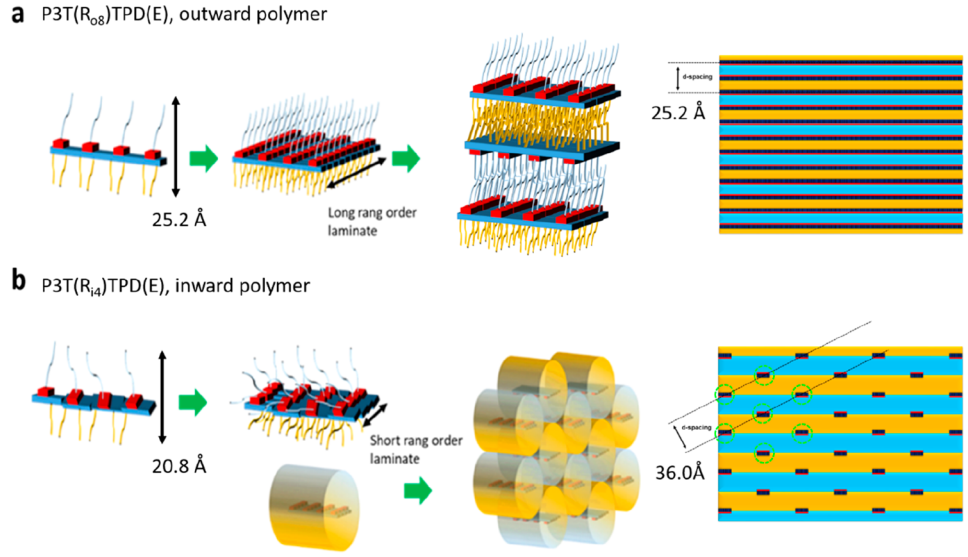

Figure 6. Structure formation mechanisms of self-assembly of P3TTPDs: (a) P3T(R$_{o8}$)TPD(E) and (b) P3T(R$_{i4}$)TPD(E) with lamellae structure and hexagonal structure, respectively, where blue line, yellow line, red box, and blue box represent TEG chain, alkyl chain, imide group on TPD unit, and thiophene unit, respectively. The *d*-spacing is calculated from the width of polymer chain based on this model.

chains provide better chain mobility of polymer to form higher ordered laminates as compared with shorter side chains[37] (Figure 6a). The far right sketch of Figure 6a is a proposed cross-sectional view of the LAM according to this model. According to the molecular simulation of P3T(R$_{o8}$)TPD(E), the calculated width of a single molecule is 25.2 Å. Then the calculated *d*-spacing should be 25.2 Å as well if all of the side chains are fully extended. The measured datum of 19.0 Å from GIWAXS indicates that the side chains are interdigitated in the lamellae layer (Supporting Information). The formation curvature HEX for conducting polymer is rather unusual.[38] Then, why do we observe it in the inward series polymers? For inward series polymers with poor coplanarity in the backbone, thus only a few backbones of the polymers can pack into a short-range lamellar layer. In addition, because of their twisted backbone, the hydrophilic TEG side chains and hydrophobic dodecyl side chains around the polymer backbones are segregated and self-assembled into cylinder and further into hexagonal structure (Figure 6b). The far right sketch of Figure 6b is a proposed cross-sectional view according to this model. According to the molecular simulation of P3T(R$_{i4}$)TPD(E), the width of single molecule is 20.8 Å. Then the calculated *d*-spacing is 36.0 Å, which is within the range of measured datum of 33.4 Å from GIWAXS (Supporting Information). Furthermore, all of side chains on the inward series polymers are compressed in the cylinders with little room for them to stick out. Thus, the shorter alkyl side chains provide a larger free volume to form highly ordered hexagonal structure as compared with the longer alkyl side chain.

CONCLUSIONS

We successfully synthesized eight 3T-TPD based CPs with different side chain location (outward and inward), type (dodecyl and TEG), and length (octyl, hexyl, and butyl). Their optical properties, electrochemical properties, thermal properties, and self-assembly behavior have been systematically studied. For the side chain location effect, the outward series polymers show a longer wavelength of λ_{max} of UV−vis absorption and obvious melting behavior than the inward series polymers. These results indicate that the outward series polymers pack better than inward series polymers and display self-assembled LAM. However, interestingly, the inward series polymers self-assemble into high order of HEX which is rarely found in D−A CPs. Forthe side chain type effect, both the outward series polymers and inward series polymers with TEG chains show a longer wavelength of λ_{max} of UV−vis absorption and higher order of the nanostructure than the polymers with dodecyl chains. These results reveal that the more flexible TEG chain can enhance the self-assembly behavior of the polymers. For the side chain length effect, the outward series polymers have a higher order of LAM with a longer side chain. On the contrary, shorter side chain is more suitable for inward series polymers to self-assemble into higher order of HEX. Finally, we purposed two models to explain the formation mechanism of LAM and HEX. This study provides a new strategy to design new D−A CPs with highly ordered nanostructure for potential application in optoelectronic devices or sensors.

ASSOCIATED CONTENT

Supporting Information

The Supporting Information is available free of charge on the ACS Publications website at DOI: 10.1021/acs.macromol.8b01073.

Synthesis method, experiment method, results of molecular orbital computation, AFM images, TGA profiles, DSC profiles, ^{1}H NMR for all synthetic intermediate and monomers (PDF)

AUTHOR INFORMATION

Corresponding Author

*E-mail suwf@ntu.edu.tw (W.-F.S.).

ORCID

Shih-Huang Tung: 0000-0002-6787-4955

Wei-Fang Su: 0000-0002-3375-4664

Notes

The authors declare no competing financial interest.

DOI: 10.1021/acs.macromol.8b01073
Macromolecules 2018, 51, 7828−7835

■ ACKNOWLEDGMENTS

The authors thank the Ministry of Science and Technology of Taiwan (106-2221-E-002-192 and 107-3017-F-002-001) and Ministry of Education (107L9006) for the financial support of this research and also thank the National Synchrotron Radiation Research Center of Taiwan for providing the GIWAXS instrument.

■ REFERENCES

(1) Tipnis, R.; Bernkopf, J.; Jia, S.; Krieg, J.; Li, S.; Storch, M.; Laird, D. Large-area organic photovoltaic module—Fabrication and performance. *Sol. Energy Mater. Sol. Cells* **2009**, *93* (4), 442−446.

(2) Krebs, F. C. Polymer solar cell modules prepared using roll-to-roll methods: Knife-over-edge coating, slot-die coating and screen printing. *Sol. Energy Mater. Sol. Cells* **2009**, *93* (4), 465−475.

(3) Scharber, M. C.; Sariciftci, N. S. Efficiency of bulk-heterojunction organic solar cells. *Prog. Polym. Sci.* **2013**, *38* (12), 1929−1940.

(4) Günes, S.; Neugebauer, H.; Sariciftci, N. S. Conjugated Polymer-Based Organic Solar Cells. *Chem. Rev.* **2007**, *107* (4), 1324−1338.

(5) Espinosa, N.; Hösel, M.; Angmo, D.; Krebs, F. C. Solar cells with one-day energy payback for the factories of the future. *Energy Environ. Sci.* **2012**, *5* (1), 5117−5132.

(6) Ma, Z.; Sun, W.; Himmelberger, S.; Vandewal, K.; Tang, Z.; Bergqvist, J.; Salleo, A.; Andreasen, J. W.; Inganas, O.; Andersson, M. R.; Muller, C.; Zhang, F.; Wang, E. Structure-property relationships of oligothiophene-isoindigo polymers for efficient bulk-heterojunction solar cells. *Energy Environ. Sci.* **2014**, *7* (1), 361−369.

(7) Ye, L.; Zhang, S.; Zhao, W.; Yao, H.; Hou, J. Highly Efficient 2D-Conjugated Benzodithiophene-Based Photovoltaic Polymer with Linear Alkylthio Side Chain. *Chem. Mater.* **2014**, *26* (12), 3603−3605.

(8) Chen, W.; Xiao, M.; Han, L.; Zhang, J.; Jiang, H.; Gu, C.; Shen, W.; Yang, R. Unsubstituted Benzodithiophene-Based Conjugated Polymers for High-Performance Organic Field-Effect Transistors and Organic Solar Cells. *ACS Appl. Mater. Interfaces* **2016**, *8* (30), 19665−19671.

(9) Zhang, M.; Tsao, H. N.; Pisula, W.; Yang, C.; Mishra, A. K.; Müllen, K. Field-Effect Transistors Based on a Benzothiadiazole−Cyclopentadithiophene Copolymer. *J. Am. Chem. Soc.* **2007**, *129* (12), 3472−3473.

(10) Sharma, B.; Sarothia, Y.; Singh, R.; Kan, Z.; Keivanidis, P. E.; Jacob, J. Synthesis and characterization of light-absorbing cyclopentadithiophene-based donor−acceptor copolymers. *Polym. Int.* **2016**, *65* (1), 57−65.

(11) Kronemeijer, A. J.; Gili, E.; Shahid, M.; Rivnay, J.; Salleo, A.; Heeney, M.; Sirringhaus, H. A Selenophene-Based Low-Bandgap Donor−Acceptor Polymer Leading to Fast Ambipolar Logic. *Adv. Mater.* **2012**, *24* (12), 1558−1565.

(12) Lee, Y. N.; Attri, P.; Kim, S. S.; Lee, S. J.; Kim, J. H.; Cho, T. J.; Kim, I. T. Photovoltaic properties of novel thiophene- and selenophene-based conjugated low bandgap polymers: a comparative study. *New J. Chem.* **2017**, *41* (14), 6315−6321.

(13) Zotti, G.; Schiavon, G.; Zecchin, S.; Morin, J.-F.; Leclerc, M. Electrochemical, Conductive, and Magnetic Properties of 2,7-Carbazole-Based Conjugated Polymers. *Macromolecules* **2002**, *35* (6), 2122−2128.

(14) Wang, N.; Chen, Z.; Wei, W.; Jiang, Z. Fluorinated Benzothiadiazole-Based Conjugated Polymers for High-Performance Polymer Solar Cells without Any Processing Additives or Post-treatments. *J. Am. Chem. Soc.* **2013**, *135* (45), 17060−17068.

(15) Ho, C.-C.; Chen, C.-A.; Chang, C.-Y.; Darling, S. B.; Su, W.-F. Isoindigo-based copolymers for polymer solar cells with efficiency over 7%. *J. Mater. Chem. A* **2014**, *2* (21), 8026−8032.

(16) Ha, J. S.; Kim, K. H.; Choi, D. H. 2,5-Bis(2-octyldodecyl)-pyrrolo[3,4-c]pyrrole-1,4-(2H,5H)-dione-Based Donor−Acceptor Alternating Copolymer Bearing 5,5′-Di(thiophen-2-yl)-2,2′-biselenophene Exhibiting 1.5 cm2·V−1·s−1 Hole Mobility in Thin-Film Transistors. *J. Am. Chem. Soc.* **2011**, *133* (27), 10364−10367.

(17) Zhou, N.; Guo, X.; Ortiz, R. P.; Harschneck, T.; Manley, E. F.; Lou, S. J.; Hartnett, P. E.; Yu, X.; Horwitz, N. E.; Burrezo, P. M.; Aldrich, T. J.; López Navarrete, J. T.; Wasielewski, M. R.; Chen, L. X.; Chang, R. P. H.; Facchetti, A.; Marks, T. J. Marked Consequences of Systematic Oligothiophene Catenation in Thieno[3,4-c]pyrrole-4,6-dione and Bithiopheneimide Photovoltaic Copolymers. *J. Am. Chem. Soc.* **2015**, *137* (39), 12565−12579.

(18) Guo, X.; Zhou, N.; Lou, S. J.; Smith, J.; Tice, D. B.; Hennek, J. W.; Ortiz, R. P.; Navarrete, J. T. L.; Li, S.; Strzalka, J.; Chen, L. X.; Chang, R. P. H.; Facchetti, A.; Marks, T. J. Polymer solar cells with enhanced fill factors. *Nat. Photonics* **2013**, *7*, 825.

(19) Zhou, N.; Guo, X.; Ortiz, R. P.; Li, S.; Zhang, S.; Chang, R. P. H.; Facchetti, A.; Marks, T. J. Bithiophene Imide and Benzodithiophene Copolymers for Efficient Inverted Polymer Solar Cells. *Adv. Mater.* **2012**, *24* (17), 2242−2248.

(20) Guo, X.; Ortiz, R. P.; Zheng, Y.; Hu, Y.; Noh, Y.-Y.; Baeg, K.-J.; Facchetti, A.; Marks, T. J. Bithiophene-Imide-Based Polymeric Semiconductors for Field-Effect Transistors: Synthesis, Structure−Property Correlations, Charge Carrier Polarity, and Device Stability. *J. Am. Chem. Soc.* **2011**, *133* (5), 1405−1418.

(21) Zhou, H.; Yang, L.; Xiao, S.; Liu, S.; You, W. Donor−Acceptor Polymers Incorporating Alkylated Dithienylbenzothiadiazole for Bulk Heterojunction Solar Cells: Pronounced Effect of Positioning Alkyl Chains. *Macromolecules* **2010**, *43* (2), 811−820.

(22) Matthews, J. R.; Niu, W.; Tandia, A.; Wallace, A. L.; Hu, J.; Lee, W.-Y.; Giri, G.; Mannsfeld, S. C. B.; Xie, Y.; Cai, S.; Fong, H. H.; Bao, Z.; He, M. Scalable Synthesis of Fused Thiophene-Diketopyrrolopyrrole Semiconducting Polymers Processed from Nonchlorinated Solvents into High Performance Thin Film Transistors. *Chem. Mater.* **2013**, *25* (5), 782−789.

(23) Duarte, A.; Pu, K.-Y.; Liu, B.; Bazan, G. C. Recent Advances in Conjugated Polyelectrolytes for Emerging Optoelectronic Applications. *Chem. Mater.* **2011**, *23* (3), 501−515.

(24) Yan, H.; Chen, Z.; Zheng, Y.; Newman, C.; Quinn, J. R.; Dotz, F.; Kastler, M.; Facchetti, A. A high-mobility electron-transporting polymer for printed transistors. *Nature* **2009**, *457* (7230), 679−686.

(25) Yang, S.-F.; Liu, Z.-T.; Cai, Z.-X.; Dyson, M. J.; Stingelin, N.; Chen, W.; Ju, H.-J.; Zhang, G.-X.; Zhang, D.-Q. Diketopyrrolopyrrole-Based Conjugated Polymer Entailing Triethylene Glycols as Side Chains with High Thin-Film Charge Mobility without Post-Treatments. *Advanced Science* **2017**, *4* (8), 1700048.

(26) Nguyen, L. H.; Hoppe, H.; Erb, T.; Günes, S.; Gobsch, G.; Sariciftci, N. S. Effects of Annealing on the Nanomorphology and Performance of Poly(alkylthiophene):Fullerene Bulk-Heterojunction Solar Cells. *Adv. Funct. Mater.* **2007**, *17* (7), 1071−1078.

(27) Gadisa, A.; Oosterbaan, W. D.; Vandewal, K.; Bolsée, J.-C.; Bertho, S.; D'Haen, J.; Lutsen, L.; Vanderzande, D.; Manca, J. V. Effect of Alkyl Side-Chain Length on Photovoltaic Properties of Poly(3-alkylthiophene)/PCBM Bulk Heterojunctions. *Adv. Funct. Mater.* **2009**, *19* (20), 3300−3306.

(28) Darling, S. B.; Sternberg, M. Importance of Side Chains and Backbone Length in Defect Modeling of Poly(3-alkylthiophenes). *J. Phys. Chem. B* **2009**, *113* (18), 6215−6218.

(29) Shi, C.; Yao, Y.; Yang; Pei, Q. Regioregular Copolymers of 3-Alkoxythiophene and Their Photovoltaic Application. *J. Am. Chem. Soc.* **2006**, *128* (27), 8980−8986.

(30) Lee, E.; Hammer, B.; Kim, J.-K.; Page, Z.; Emrick, T.; Hayward, R. C. Hierarchical Helical Assembly of Conjugated Poly(3-hexylthiophene)-*block*-poly(3-triethylene glycol thiophene) Diblock Copolymers. *J. Am. Chem. Soc.* **2011**, *133* (27), 10390−10393.

(31) Yao, K.; Chen, L.; Chen, X.; Chen, Y. Self-Organized Hole Transport Layers Based on Polythiophene Diblock Copolymers for Inverted Organic Solar Cells with High Efficiency. *Chem. Mater.* **2013**, *25* (6), 897−904.

(32) Cheng, Y.-J.; Cao, F.-Y.; Lin, W.-C.; Chen, C.-H.; Hsieh, C.-H. Self-Assembled and Cross-Linked Fullerene Interlayer on Titanium

DOI: 10.1021/acs.macromol.8b01073
Macromolecules 2018, 51, 7828−7835

Oxide for Highly Efficient Inverted Polymer Solar Cells. *Chem. Mater.* **2011**, *23* (6), 1512−1518.
(33) Ouattara, M. P.; Lenfant, S.; Vuillaume, D.; Pézolet, M.; Rioux-Dubé, J.-F.; Brisson, J.; Leclerc, M. Langmuir−Blodgett Films of Amphiphilic Thieno[3,4-c]pyrrole-4,6-dione-Based Alternating Copolymers. *Macromolecules* **2013**, *46* (16), 6408−6418.
(34) Zhang, S.; Gao, J.; Wang, W.; Zhan, C.; Xiao, S.; Shi, Z.; You, W. Effect of Replacing Alkyl Side Chains with Triethylene Glycols on Photovoltaic Properties of Easily Accessible Fluorene-Based Non-Fullerene Molecular Acceptors: Improve or Deteriorate? *ACS Applied Energy Materials* **2018**, *1* (3), 1276−1285.
(35) Mei, J.; Kim, D. H.; Ayzner, A. L.; Toney, M. F.; Bao, Z. Siloxane-Terminated Solubilizing Side Chains: Bringing Conjugated Polymer Backbones Closer and Boosting Hole Mobilities in Thin-Film Transistors. *J. Am. Chem. Soc.* **2011**, *133* (50), 20130−20133.
(36) Lee, J.; Han, A. R.; Kim, J.; Kim, Y.; Oh, J. H.; Yang, C. Solution-Processable Ambipolar Diketopyrrolopyrrole−Selenophene Polymer with Unprecedentedly High Hole and Electron Mobilities. *J. Am. Chem. Soc.* **2012**, *134* (51), 20713−20721.
(37) Back, J. Y.; An, T. K.; Cheon, Y. R.; Cha, H.; Jang, J.; Kim, Y.; Baek, Y.; Chung, D. S.; Kwon, S.-K.; Park, C. E.; Kim, Y.-H. Alkyl Chain Length Dependence of the Field-Effect Mobility in Novel Anthracene Derivatives. *ACS Appl. Mater. Interfaces* **2015**, *7* (1), 351−358.
(38) Ko, S.; Kim, D. H.; Ayzner, A. L.; Mannsfeld, S. C. B.; Verploegen, E.; Nardes, A. M.; Kopidakis, N.; Toney, M. F.; Bao, Z. Thermotropic Phase Transition of Benzodithiophene Copolymer Thin Films and Its Impact on Electrical and Photovoltaic Characteristics. *Chem. Mater.* **2015**, *27* (4), 1223−1232.

DOI: 10.1021/acs.macromol.8b01073
Macromolecules 2018, 51, 7828−7835